Progress in Natural Science: Materials International 2013;23(3):245–255

Chinese Materials Research Society

Progress in Natural Science: Materials International

www.elsevier.com/locate/pnsmi
www.sciencedirect.com

REVIEW

Understanding supercapacitors based on nano-hybrid materials with interfacial conjugation

George Z. Chen

Department of Chemical and Environmental Engineering, and Energy and Sustainability Research Division, Faculty of Engineering, University of Nottingham, Nottingham NG7 2RD, UK

Received 26 November 2012; accepted 20 March 2013
Available online 18 May 2013

KEYWORDS

Supercapacitors;
Carbon nanotubes;
Graphenes;
Electronically conducting polymers;
Transition metal oxides;
Interfacial conjugation

Abstract The recent fast development of supercapacitors, also known scientifically as electrochemical capacitors, has benefited significantly from synthesis, characterisations and electrochemistry of nanomaterials. Herein, the principle of supercapacitors is explained in terms of performance characteristics and charge storage mechanisms, i.e. double layer (or interfacial) capacitance and pseudo-capacitance. The semiconductor band model is applied to qualitatively account for the pseudo-capacitance in association with rectangular cyclic voltammograms (CVs) and linear galvanostatic charging and discharging plots (GCDs), aiming to differentiate supercapacitors from rechargeable batteries. The invalidity of using peak shaped CVs and non-linear GCDs for capacitance measurement is highlighted. A selective review is given to the nano-hybrid materials between carbon nanotubes and redox active materials such as electronically conducting polymers and transition metal oxides. A new concept, "interfacial conjugation", is introduced to reflect the capacitance enhancement resulting from π–π stacking interactions at the interface between two materials with highly conjugated chemical bonds. The prospects of carbon nanotubes and graphenes for supercapacitor applications are briefly compared and discussed. Hopefully, this article can help readers to understand supercapacitors and nano-hybrid materials so that further developments in materials design and synthesis, and device engineering can be more efficient and objective.

© 2013 Chinese Materials Research Society. Production and hosting by Elsevier B.V. All rights reserved.

1. Introduction

The foreseeable exhaustion of fossil resources is calling for development of technologies that can enable either or both of (1) greater efficiency of energy consumption and (2) reliable utilisation of renewable energy. These needs are not only for mitigation of the negative environmental impact of CO_2 emission from fossil fuel combustion, but more importantly for the security of sustained

E-mail address: george.chen@nottingham.ac.uk
Peer review under responsibility of Chinese Materials Research Society.

ELSEVIER Production and hosting by Elsevier

1002-0071 © 2013 Chinese Materials Research Society. Production and hosting by Elsevier B.V. All rights reserved.
http://dx.doi.org/10.1016/j.pnsc.2013.04.001

energy supply when fossil resources run out or become too expensive to use. Energy efficiency can be improved in various existing technologies. For example, elevators are the necessity in high buildings. Energy input is needed to raise the elevator against gravity, and the rising process accumulates potential energy. It is obviously desirable to convert the potential energy to a storable and reusable form during the downward course of the elevator. The stored energy can then be released to assist lifting the elevator, and hence improve energy efficiency. Obviously, to match the relatively fast movement of the elevator, the energy storage system must be capable of charging and discharging quickly.

The solution has been recognised to be a fast electrochemical energy storage device, i.e. the supercapacitor which will be discussed in detail in Section 2. An early case study showed that the maximum power demand to operate a medium sized elevator with full load (3500 kg, 10 floors) would be, respectively, 33 kW without, but 2.5 kW with the incorporation of a supercapacitor system [1]. In principle, this energy saving strategy can be applied to many other similar devices that repeatedly lift and lower heavy objects. On the other hand, more energy efficient technologies can also help the acceptance of renewable energy which is at present expensive to harvest and convert to a usable form. Although the cost for harvesting and conversion of renewable energy may decrease with technology improvement, the intermittency of various forms of renewable sources still requires energy storage to ensure continuous and stable supply. Therefore, energy conversion and storage at various scales (kWh~GWh per unit system) is needed so that efficient, reliable and affordable energy supply can be achieved in the post-fossil era.

In fact, energy conversion and storage is a historical topic of research and commercial efforts, and existing technologies range from "pumped storage hydroelectricity" at MWh or greater scales to rechargeable batteries with capacities as small as mWh. The driver for continuous development of various energy conversion and storage technologies was and still is the cost resulting from, for example, resources availability, active materials synthesis, device manufacture, energy capacity, power capability, provision reliability, service life, environmental impact and recyclability. It is unlikely for any single technology, disregarding however advanced it is, to win over others on all these aspects. The more realistic solution to secure reliable and affordable energy supply in the post-fossil era can only be a combination of various technologies.

For the same reason, this article is not intended to compare and comment on the advantages and disadvantages of various existing and emerging energy conversion and storage technologies. Instead, the author will briefly review recent research development as reported in the literature, mostly from the author's own laboratory, on one of the emerging technologies, namely supercapacitor whose fast development in recent years has largely benefited from the use of appropriate nanomaterials. A particular attention is given to the basics of supercapacitor and its difference from a common rechargeable battery. The author also hopes that this article can help better understanding of the energy storage mechanisms and the performance characteristics of supercapacitors in terms of their similarities to and differences from the more widely known rechargeable batteries.

2. Supercapacitor basics

Understanding of the supercapacitor may be easier by comparing it with the conventional capacitors that are widely used in electronic devices. There are two types of conventional capacitors, both of which are composed of a positive electrode plate, a negative electrode plate and, between the two plates, a dielectric or ionic medium which must be non-conductive to electrons. In the first type of capacitors, the medium is a dielectric material, such mica, in which the dipoles can be polarised to accumulate electric charge (Q) at the interface between the electrode plate and the dielectric medium. In the second type of capacitors, the medium is a liquid or solid ionic conductor which is also often called electrolyte. In such a case, charge storage is achieved by accumulation of positive ions (cations) at the interface between the negative electrode and the electrolyte, and negative ions (anions) of an equal amount of charge at the interface between the negative electrode and the electrolyte. Fig. 1 illustrates the solid dielectric capacitor (a) and the liquid electrolytic capacitor (b).

It is worth emphasising again that both the dielectric and electrolytic media are insulators to electrons. An important feature of the electrolytic capacitor is that the ions are freely mobile in the electrolyte bulk. Thus, in principle, when the positive charge density on the electrode side is increased, an equal amount of negative charge can accumulate on the electrolyte side via "packing" of anions on the surface of the electrode. On the contrary, in the dielectric capacitor, the dipoles are non-mobile in the solid dielectric medium, and the positive and negative charges in the dipoles are always associated and arranged in an alternative manner as shown in Fig. 1a. Thus, a much greater charge density can be achieved at the electrode/electrolyte interface than at the electrode/dielectric interface. For this reason, the capacitance is often in the mF range for electrolyte capacitors, but in the μF range for dielectric capacitors.

In both dielectric and electrolytic capacitors, the amount of charge stored is in proportion to the strength of the applied electric field or the voltage (U) between the positive and negative plates.

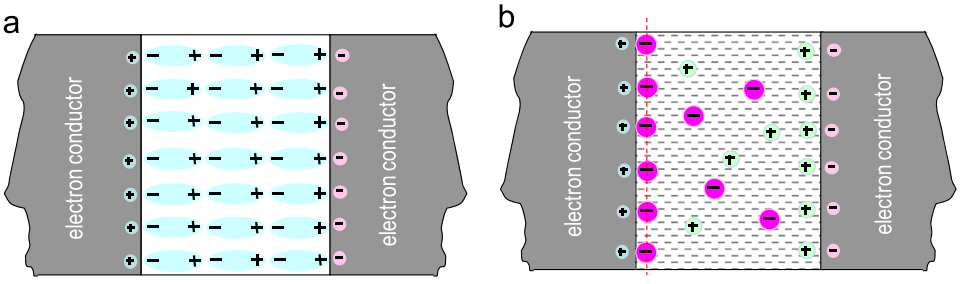

Fig. 1 Schematic illustration of charge storage in conventional capacitors with (a) a solid dielectric medium where the non-mobile dipoles are alternatively arranged in terms of charge distribution, or (b) a liquid or solid electrolyte with freely mobile ions in the bulk, but packed ions in the electrolyte side next to the electrode surfaces.

The proportionality is called capacitance (C) which links Q and U according to Eq. (1) below.

$$C = \frac{Q}{U} = \frac{\varepsilon_0 \varepsilon A}{d} \tag{1}$$

C is a function of the dielectric constant (or relative permittivity, ε) of the dielectric medium, and proportional to the ratio of the area of the electrode/dielectric interface (A) and the separation distance between the two electrode plates (d). ε_0 ($=8.854 \times 10^{-12}$ F/m) is the vacuum permittivity.

Eq. (1) can be mathematically converted into different forms to fit with different experimental tests. The most relevant test is the current response to the voltage variation as can be derived by rearranging Eq. (1) to $Q=CU$ which can be differentiated against time to give the following equation, considering that C is a constant.

$$\frac{dQ}{dt} = C\frac{dU}{dt} + U\frac{dC}{dt} = C\frac{dU}{dt} \tag{2}$$

If the applied voltage varies linearly with time, i.e. $U=U^o+vt$, where t is the time, U^o is the starting voltage which may be zero, and v is the voltage scan rate, then, $dU/dt=v$. (In a three electrode cell as discussed in more detail below, the voltage is replaced by the electrode potential, and v is called the potential scan rate). Considering that $dQ/dt=i$ (current), Eq. (2) can be further simplified to correlate the current with the scan rate.

$$i = Cv \tag{3}$$

Eq. (3) shows that the current, i, flowing through a capacitor is proportional to the linear variation rate of the voltage, v, but independent of U itself. Note that v is positive for increasing voltage, or negative for decreasing voltage. As a result, the current can also be positive or negative, depending on the direction of the voltage scan. Particularly, if the voltage scan is suddenly reversed in direction but retains the same rate, the current will jump from a positive value to a negative value. This feature of Eq. (3) gives the rectangular i–U plots at different voltage scan rates as shown in Fig. 2a. In fact, the rectangular shape of the i–U plot, which is also known as cyclic voltammogram (CV), is an experimental criterion for qualitatively judging capacitive behaviour of a device or electrode made from a synthetic pure or composite material of interest.

On the other hand, if a constant current is applied to charge (positive current) or discharge (negative current) the capacitor, Eq. (3) predicts a constant rate of voltage increase (charging) or decrease (discharging). Thus, if the voltage of the capacitor is plotted against the time during a cycle of constant current charging and discharging, which is actually the integration of Eq. (3), a triangular curve is expected as shown in Fig. 2b. Note that constant current charging–discharging is also known as galvanostatic charging–discharging (GCD).

A capacitor is capable of storing electric energy. When a voltage, U, is applied to the capacitor for a short time, a small amount of work, dW, is done to move a small quantity of charge, dQ, to be accumulated at the electrode/dielectric medium interface. This small amount of work is the product of the voltage and charge, i.e. $dW=UdQ$. Assuming an insignificant heat loss, dW is equivalent to the amount of energy stored in the capacitor, and can be linked to Eq. (1) to give the following equations after integration.

$$dW = UdQ = \frac{Q}{C}dQ \tag{4}$$

$$W = \int_0^Q \frac{Q}{C}dQ = \frac{1}{2}\frac{Q^2}{C} = \frac{QU}{2} = \frac{CU^2}{2} \tag{5}$$

It is worth mentioning that Eq. (1) shows that the voltage of a capacitor is proportional to the amount of charge accumulated in the capacitor. Also, a practical capacitor has always a maximum tolerable voltage, U_{max}, beyond which the dielectric or ionic medium will break down (or decompose). Because C is determined by the dielectric material used, a capacitor can only store a maximum amount of energy limited by the value of U_{max} as defined by Eq. (5).

The power output, P, from a capacitor can be in principle derived from dividing W by t, the time needed to fully discharge the capacitor, i.e.

$$P = \frac{W}{t} = \frac{CU^2}{2t} \tag{6}$$

Obviously, the maximum power output is determined by the shortest discharging time, which cannot be derived from any of the equations above.

It is a fact that any electric power source has an internal resistance known as the equivalent series resistance, or simply ESR. Assuming the power source is connected to a load, R_L, through the circuit shown in Fig. 3. Given the voltage of the power source as U, the current passing through the circuit is $i=U/R$, where $R=R_L$+ESR. The power transferred from the source to the load is $P=iU=i^2R_L$. Then, Eq. (7) below can be derived.

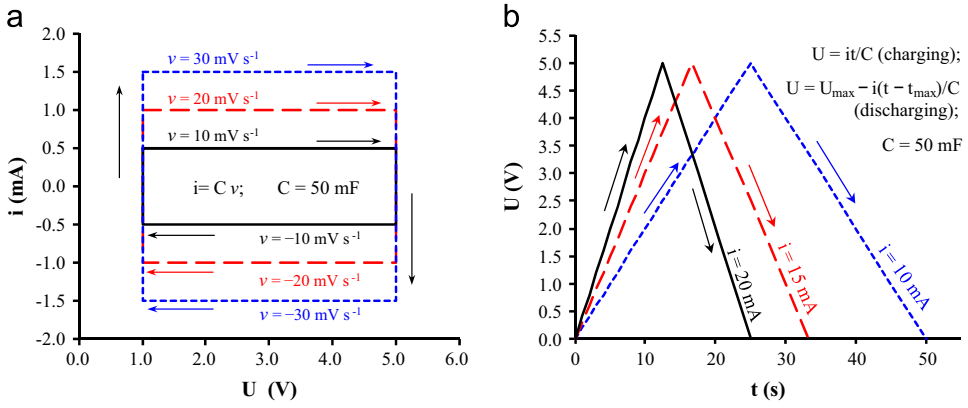

Fig. 2 (a) CVs at indicated voltage scan rates, and (b) GCD plots at indicated constant currents as derived from Eq. (3) for a 50 mF capacitor with $U_{max}=5$ V. In the GCD plots in (b), $t_{max}=U_{max}C/i$.

$$P = \left(\frac{U}{R_L + \mathrm{ESR}}\right)^2 R_\mathrm{L} = \frac{R_\mathrm{L} U^2}{(R_L + \mathrm{ESR})^2} \tag{7}$$

Eq. (7) shows that the maximum power, P_{max}, can be reached at $R_L = \mathrm{ESR}$, i.e.

$$P_{max} = \frac{\mathrm{ESR}U^2}{(\mathrm{ESR} + \mathrm{ESR})^2} = \frac{U^2}{4\mathrm{ESR}} \tag{8}$$

It is interesting to note that Eq. (8) shows that P_{max} is a function of U and ESR, but independent of C, although C determines the amount of energy stored in the capacitor. However, the shortest discharging time, t_{min}, can be derived by bringing Eq. (8) into Eq. (6).

$$t_{min} = \frac{CU^2}{2P_{max}} = \frac{CU^2}{2(U^2/4\mathrm{ESR})} = 2C\mathrm{ESR} \tag{9}$$

The above equation should be practically very useful and important for designing supercapacitor supported systems. However, the current literature has been mostly reporting data and analyses in relation with Eq. (8), whilst almost no attention or recognition has been placed on Eq. (9). This is somehow unfortunate because highlighting the maximum power of supercapacitors against that of batteries without mentioning the lasting time the device can work at the high power may confuse or even mislead readers and customers who are not well informed.

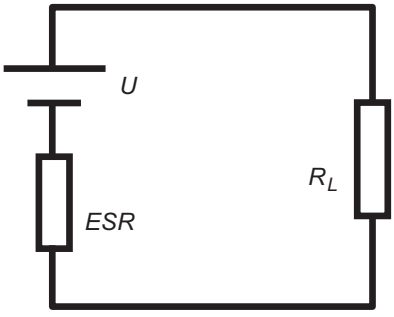

Fig. 3 A simple electric circuit connecting a power source (U) with a working load (R) via an equivalent series resistance (ESR) of the power source. This circuit is used to derive Eqs. (8) and (9).

3. Performance differences between supercapacitor and rechargeable battery

The capacitance of a conventional capacitor typically ranges between 10^{-6} and 10^{-2} F, but commercial supercapacitors are commonly rated at 10^{2}–10^{4} F. However, this huge difference in capacitance does not change the fact that a supercapacitor is still a capacitor. Thus, the behaviour of a supercapacitor should also be governed by all the equations discussed in Section 2 with the CV and GCD plots being the same as those shown in Fig. 2a and 2b, respectively.

In practice, most supercapacitors with activated carbon, carbon nanotubes or graphenes as the electrode materials behave closely to that shown in Fig. 2. However, if redox active materials such as some transition metal oxides (TMOs) and electronically conducting polymers (ECPs) are used to make the electrodes, it is not uncommon that the device behaves with a certain degree of deviation from an ideal capacitor.

Redox active materials can store electric charge via electron transfer or Faradaic reactions. The CV or GCD plots of a Faradaic reaction may follow closely to those shown in Fig. 2, giving rise to the so called **pseudo-capacitance**. On the other hand, Faradaic reactions are also responsible for charge storage in rechargeable batteries which however do not produce rectangular CVs or triangular GCDs. Instead, battery electrodes show typically oxidation and reduction current peaks on the CV, or potential plateaux on the GCD plot over a narrow potential range due to the strong dependence of the electrode reaction on electrode potential. Fig. 4a and b displays the CVs and GCD plots of a hypothetical positive battery electrode on which the Faradaic reaction is reversible, as reflected by the symmetrical shapes of the CVs (horizontal axis) and GCDs (vertical axis).

However, in almost all commercial batteries, the electrode reactions are much less reversible due to various polarisations resulting from, for example, kinetic barriers for electron transfer, ohmic resistance and ion transport difficulty. As a result, the CV of the positive electrode would exhibit an oxidation current peak at a more positive potential than that of the reduction current peak. On the GCD plots, the charging potential plateau would appear at a more positive potential than the discharging potential plateau. The lower reversibility of electrode reactions in commercial batteries is the main cause for the lower energy efficiency.

The differences in performance are obvious between Fig. 2 for supercapacitors and Fig. 4 for batteries (with reversible electrode reactions). Nevertheless, in both cases, the interest is for energy storage. It is thus necessary to decide whether or not the difference

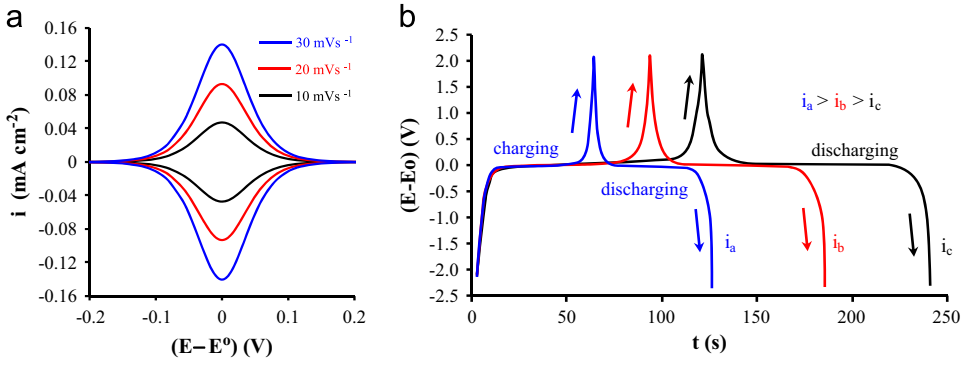

Fig. 4 (a) CVs at indicated potential scan rates, and (b) GCD plots at indicated constant currents of $i_a > i_b > i_c$ for a reversible Faradaic reaction with localised electron transfer to and from isolated redox sites on the electrode.

is affecting the validity of the equations discussed in Section 2, particularly Eq. (5) which is used to calculate the energy capacity (kJ or Wh) of the device and in turn to derive the specific energy (kJ/kg or Wh/kg) and/or energy density (kJ/L or Wh/L). [It is worth noting that, the units of kJ/kg (or Wh/kg) and kW/kg were incorrectly used for energy density and power density, respectively, by some authors. Strictly, energy density should be expressed in kJ/L or Wh/L, and power density in kW/L].

For example, using both Figs. 2 and 4, one can calculate the ratio of charge (C) and voltage (V) and obtain a quantity that has the same unit as capacitance (F). This value is indeed capacitance for Fig. 2 which is derived from a capacitor. The question is what could be wrong if the ratio is also considered to be capacitance for Fig. 4. Firstly, for Fig. 2, the charge stored or released is proportional to the voltage applied or measured but the charge/voltage ratio is a constant or independent of the voltage applied. It is very different for Fig. 4 where the charge is not proportional to the potential change, and the ratio of charge/(potential change) depends strongly on the potential. It maximises at the current peak potential, but decreases rapidly when the potential moves away from the current peak potential. Secondly, the energy in a storage device can be calculated by integration of the GCD plot as shown in Eq. (5) which is proportional to the area under the GCD plot. Because the charge/voltage ratio, or in other words the capacitance is a constant over the range of applied voltages in a capacitor, the integration of the GCD plot leads to the simple energy expression, i.e. Eq. (5): $W=CU^2/2$. Obviously, if the charge/voltage ratio changes with the applied voltage, Eq. (5) is invalid for the calculation of energy. Instead, the energy has to be calculated by, for example, integration of the GCD plot.

In the literature, some authors have indeed reported the charge/voltage ratio derived from non-rectangular (or peak-shaped) CVs or non-triangular (or significantly curved) GCDs as the capacitance, and then bring this ratio into Eq. (5) to calculate the energy value. The list of such publications is too long to be given here, but Fig. 5 illustrates the problems with a peak-shaped CV and the corresponding non-linear GCD that are commonly observed on positive electrodes with a quasi-reversible Faradaic reaction [2–4].

There are two features on the CV (solid line) in Fig. 5a that reflect the quasi-reversibility of the electrode reaction. First, the CV is not symmetrical as those in Fig. 4a. The potential of the oxidation (positive) current peak is more positive than that of the reduction (negative) current peak. Second, integration of the positive current over the potential (which is a linear function of time, i.e. $E=E^o+vt$) would give a larger charge than that of the negative current. The GCD plot in Fig. 5b (solid line) is recorded in the potential range selected from the CV as indicated by the two vertical dashed lines (i.e. between 0 V and 0.8 V). It can be seen that the charging time is longer than the discharging time. Because the current is the same for charging and discharging but opposite in direction, the GCD plot indicates that only a portion of the charge passed during the charging period is released during the discharging period. This is a reflection of the electrode reaction being not fully reversible.

Clearly, the charge/voltage ratio from either the CV or GCD in Fig. 5 (here, the voltage is equivalent to the potential range between the two vertical dashed lines in Fig. 5a, or the maximum and minimum potentials in Fig. 5b) is much larger for charging than for discharging. Specifically for the GCD in Fig. 5b, the charge/voltage ratio, which is larger for charging than discharging, is the reciprocal of the slope of the dashed lines. If this ratio is considered as the capacitance and used in Eq. (5), the calculated energy is the shaded area under the dashed straight lines. However, the actual energy is the area under the curved solid lines. In other words, using the charge/voltage ratio as the capacitance, the energy calculated from Eq. (5) is underestimated for charging, but overestimated for discharging.

4. Charge storage mechanisms in electrode materials of supercapacitor

According to Eq. (1), the capacitance of a supercapacitor is proportional to the charge capacity but to the reciprocal of the voltage. For any power device, a certain level of voltage is needed to export the energy. Also, because the energy capacity of a supercapacitor is proportional to the square of the voltage according to Eq. (5), a high voltage is always desirable. Thus, to achieve high capacitance, a great effort has been made to increase the capacitance.

The initial effort was to develop porous carbon materials, e.g. activated carbons, with high specific surface area, resulting in the **first generation supercapacitors** in which charge storage occurs in the electric double layer at the electrode/electrolyte interface. This storage mechanism is the same as that in the traditional electrolytic capacitors, but the specific capacitance (F/g) increases by a factor of several orders of magnitude because of the very large specific surface area (m^2/g) of porous carbons. Although

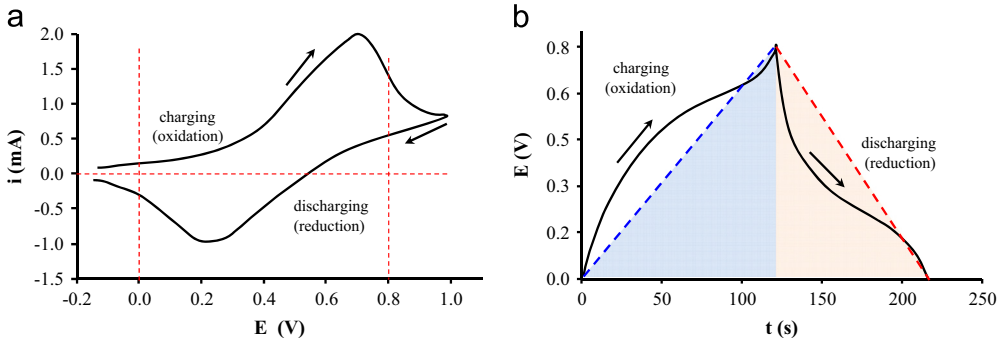

Fig. 5 Typical CVs (a) and GCDs (b) of a quasi-reversible Faradaic reaction in a redox active material (solid lines), and of a capacitive material (dashed lines). Both materials are tested as the positive electrode. The area under the current curve of the CV is proportional to the charge passed during the forward (or backward) potential scan, but the area under the potential curve of the GCD is proportional to the energy consumed (or released) during charging (or discharging).

porous carbons have been the choice for making an **electric double layer capacitor** (EDLC), there are restrictions due to the correlations between specific surface area, porosity, strength and electronic conductivity. Simply, the greater is the porosity of the carbon, the larger is the specific surface area, but the weaker and less conducting the carbon becomes. The other issue is that not all the internal surface area, such as those of the wall of micro-pores, can be accessed by ions in the activated carbon for charge storage. Thus, for activated carbons, although their specific surface areas are typically 1000–2000 m^2/g, the specific capacitance is usually smaller than 100 F/g [5].

Although the observation of high capacitance in porous carbons was included in a patent application in 1954 [6], understanding and further research on carbon based EDLCs [7] started after the first report of ruthenium dioxide exhibiting ideal capacitive properties [8]. Many redox active materials, typically transition metal oxides (TMOs) and electronically conducting polymers (ECPs), were also studied [9], leading to the second generation supercapacitors in which charge storage in the electrode involves fast and reversible electron transfer or Faradaic reactions in a wide potential range than that in a conventional battery. Such a storage mechanism is known as pseudo-capacitance. Unlike porous activated carbons which store the charge in the EDL in a two-dimensional manner, the capacitance of redox active materials is achieved via charge storage within the three-dimensional structure of the material. Thus, the specific capacitance of redox active materials is about an order of magnitude larger than that of EDL materials.

It is worth emphasising that pseudo-capacitance is Faradaic in nature, but is not, and should not be related to current peaks on CVs, although some authors unfortunately made such claims [2–4]. In terms of performance, pseudo-capacitance is the same as double layer capacitance, corresponding to rectangular CVs and triangular GCDs as those shown in Fig. 2a and b, respectively. The confusions might have resulted from poor understanding of the origin of pseudo-capacitance. A qualitative explanation was recently proposed [9,10] according to the band theory for semi-conductors and is described briefly blow with reference to Fig. 6 [11].

Electron injection to (or removal from) an electrode may occur in electronically interactive or separated redox active sites, very much depending on the conductivity of the material. Well separated (or isolated) sites should have equal or fairly close energy states, and hence accept (or donate) electrons at potentials

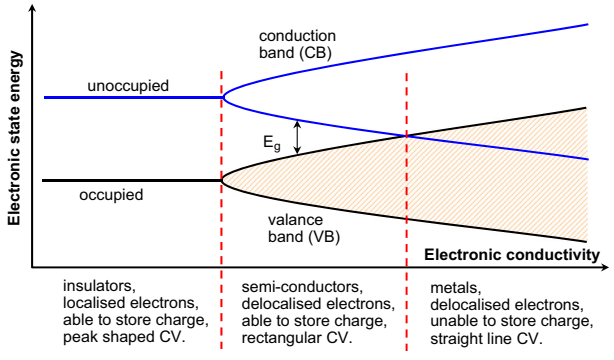

Fig. 6 Schematic representation of the band theory and its correlation with conductivity, charge storage capability and shape of different types of materials. (Note that the situation for insulators (far left) is applicable to redox active molecules or ions in a liquid solution.).

very close to each other, leading to the peak shaped CV in a narrow potential range as shown in Fig. 4a. However, if these redox active sites can interact with each other due to either short separations or good electronic conductivity or both, their energy states can merge into a broad band with negligibly small differences between the neighbouring states. Such a situation corresponds to the conduction band in semiconductors, including most TMOs, and is also comparable with the electron delocalisation in conjugated chemical bonds, as in ECPs, resulting from overlapping electron orbits between neighbouring atoms. As a result, electron transfer into (or from) each energy state in this broad band becomes continuous over a wide range of potentials, which is responsible for the constant current flow and hence the rectangular CV.

Although having larger specific capacitance, materials possessing pseudo-capacitance suffer from their semiconducting nature. In a practical supercapacitor, it is desirable to load as much as possible the active materials to maximise the energy capacity, which can be achieved by increase the coating thickness of the active material. This approach has unfortunately a very limited effect because of the high electrode resistance which not only reduces the power capability in line with Eq. (8), but also prevents electronic access to all active sites inside the thick coating.

Another challenge to pseudo-capacitive materials is for charge balancing ions to access the active sites inside the semiconducting material, particularly in the form of a thick coating, due to slow solid state diffusion. The consequences are significantly compromised specific capacitance and power capability. Actually, there is a more serious problem in association with the required access by ions in pseudo-capacitive materials. Repeated ingression and depletion of ions in the electrode material cause inevitably cyclic stress changes at microscopic levels, leading to structural alteration or even disintegration around the active sites. For this reason, the cyclic charging–discharging life of a pseudo-capacitor ($\sim 10^3$ cycles) is much shorter than that of an EDLC ($> 10^5$ cycles).

5. Nanostructure enhanced performance of pseudo-capacitive materials

The influence of slow solid state diffusion of ions on capacitive performance is generally insignificant in thin layer materials for short times. Particularly, if the thin layer is made from nanomaterials, more active sites would be located on or near the surface. Therefore, access by the charge balancing ions require no or only shallow solid state diffusion. In the past decades, it is evident in the literature that nanomaterials have been very popularly researched and developed for supercapacitor application, leading to a significant increase in the specific capacitance (F/g) [9]. However, it is also true that if such a nanostructured pseudo-capacitive material was made into a thicker film (e.g. above 10 mg/cm^2 in loading), the performance would deteriorate very quickly. The dilemma is to minimise the contact resistance between the nano-particulates, but also maintain sufficient and selective particle separation to provide channels amongst the nano-particulates for liquid electrolyte access and ion transport.

An effective approach to overcome the electronic and ionic drawbacks arising from packing pseudo-capacitive nano-particulates into thick films is to hybridise them with an appropriate carbon based nano-material which can offer sufficient electronic conductivity. The author and co-workers succeeded to coat carbon nanotubes (CNTs) individually with a thin layer (e.g. 10–100 nm

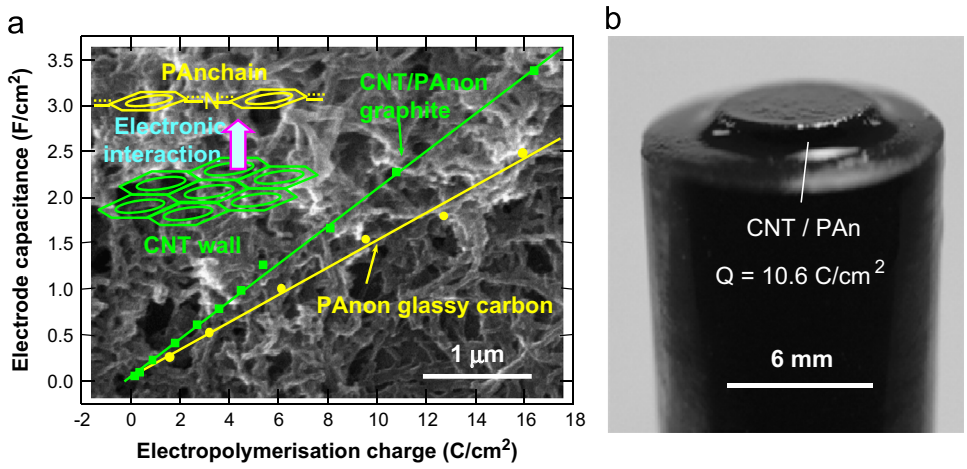

Fig. 7 (a) SEM image of the microstructure of the surface of an electro-deposited CNT/PAn film. The superimposed plots show the electrode capacitance varying proportionally to the deposition charge for CNT/PAn (green marks and line) and PAn (yellow marks and line). (b) Photograph of an epoxy-sheathed graphite electrode with a thick electro-deposited CNT/PAn coating [17,18].

thick) of different redox active materials, and reported greatly improved capacitive performance [12–16]. CNTs are highly electronically conducting, and have high aspect ratios and curved shapes. These properties can improve electronic conduction in the solid phase of the hybrid materials, and are beneficial to formation of micro- and nano-meter pores or channels between the CNTs when they are packed together.

Fig. 7a shows the surface micro-structures of an electrochemically deposited composite film of polyaniline (PAn) and CNTs, revealing clearly micro- and nano-pores formed in the well networked CNT/PAn hybrid fibrils. Also shown in Fig. 7a is the plot (green markers and linear fitting) of the capacitance of the CNT/PAn film as a linear function of electro-deposition charge which is proportional to the film thickness. For comparison, the plot for similarly prepared PAn films (yellow markers and linear fitting) is also presented, showing noticeably smaller electrode capacitance than that of the CNT/PAn films. Fig. 7b is the photograph of an electro-deposited CNT/PAn film about 0.5 mm thick. The charge used to deposit this film was slightly over 10C/cm^2. However, for PAn deposition at the same amount of charge, the film was much thinner. This difference may be explained by the inclusion of CNTs which are not only more bulky than individual polymer chains, but also rigid and curved. Thus, packing together these CNTs, with or without the surface coating, would naturally leave empty spaces between the curved nanofibrils.

6. Capacitive synergy in hybrid nanomaterials

The observed greater electrode capacitance (F/cm^2) of the CNT/PAn films than similarly prepared PAn film was initially thought to be due to CNTs having increased both the electronic and ionic conductivities of the composite films. However, this thought cannot account for the fact that the CNT–PAn composite had greater capacitance even for very thin films in which conductivity should have played an insignificant role. This phenomenon was also observed in our studies of other electro-deposited electronically conducting polymers (ECPs), such as polypyrrole (PPy) and poly[3,4-ethylene-dioxythiophene] (PEDOT), and their composites with CNTs [13,19].

One may argue that the higher electrode capacitance of the CNT/ECP films could have resulted from CNTs themselves being EDLC type materials. This contribution, however, could account only for a small part of the capacitance increase. This is because the content of CNTs in the CNT–ECP composites was typically about 20 wt% as determined by elemental analysis, and the specific capacitance of the CNTs (acid treated) was smaller than 50 F/g [17]. Thus, there must be other direct interactions between the CNTs and the coated ECPs, and two types of interactions have been identified as discussed below.

The first type is the electrostatic interaction between the positive charges along the polymer chains and the negative charges of the carboxylic groups on the surface of the CNTs. The presence of negative charges on the CNTs is further enriched by acid treatment for improved dispersion in water. The negative charges on the CNTs make the removal of electrons from the polymer easier via oxidation, which is in agreement with the negative shift of the peak potentials on the CV of CNT/PPy from that of PPy as shown in Fig. 8a and b. Further, the negatively charged CNTs are fixed (or non-mobile) inside the polymer, and cannot be removed when the polymer is reduced to its neutral state. Instead, cations have to move into the polymer to help maintain the electric neutrality in the reduced neutral polymer. This means that the redox chemistry of the ECP in the CNT composite involves not only the larger anions at more positive potentials, but also the smaller cations at less positive potentials. This prediction was confirmed experimentally, as demonstrated in Fig. 8 with the CV and the simultaneously measured mass change during the potential scan (known as cyclic voltmassograms) in a CNT–PPy film in aqueous electrolyte [20]. These CNT induced changes in charge transfer processes of the ECPs should have contributed to the observed larger electrode capacitance of the composite films as exemplified in Fig. 7a for CNT/PAn.

7. Interfacial conjugation in Hybrid nanomaterials

The second type is the $\pi-\pi$ stacking interactions. Chemical bonding in both ECPs and CNTs include highly conjugated π −bonds which are unsaturated and have still the tendency of further bonding. A typical example is the so called $\pi-\pi$ stacking

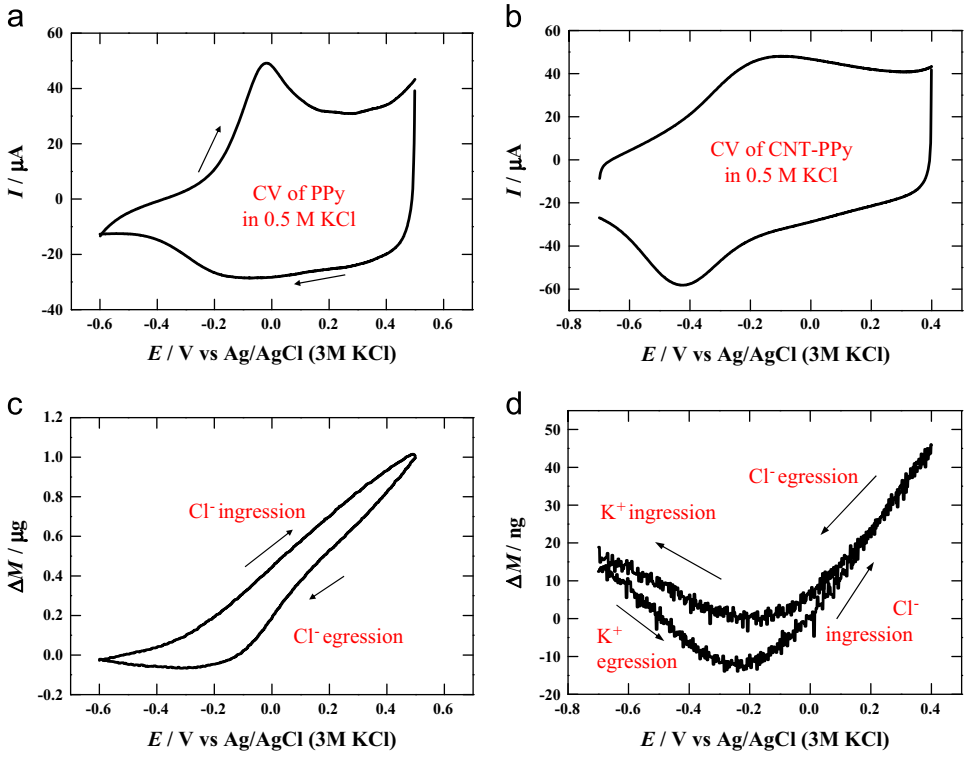

Fig. 8 CVs (a,b) and the simultaneously recorded mass changes during the potential scan (c,d) of PPy (a,c) and CNT/PPy (b,d) films in aqueous KCl solution. The plots of mass change vs potential are known as cyclic voltmassogram and were recorded on the electrochemical crystal microbalance [20].

(a form of secondary bonds) between the highly conjugated graphene sheets in graphite which is a rare example of non-metals with high electronic conductivity. Similarly, when the conjugated bonds of ECP and CNT come close to each other at the CNT/ECP interface, the $\pi-\pi$ stacking interaction takes place. This understanding is schematically illustrated in the inset of Fig. 7a where the conjugation in CNTs is represented by the graphene sheet (drawn in green), whilst that in PAn by the two monomer units (drawn in yellow). The consequence of these direct interactions between CNTs and ECPs is further delocalisation of the electrons in the conjugated bonds of the ECPs, which in turn decreases the number of monomers involved in each electron transfer. Obviously, the fewer monomer units for each electron transfer, the greater the capacity of the polymer for electron transfer. The presence of $\pi-\pi$ stacking interactions in CNT/PAn is supported by IR or FTIR spectroscopic analyses [18,21]. Because the $\pi-\pi$ interaction discussed here occurs at the interface between two conjugated systems, the author proposes to describe it as "**interfacial conjugation**".

It is worth emphasising that delocalised electrons are present not only in ECPs, but also commonly in many semiconductor type materials, specially transition metal oxides (TMOs). Thus, interfacial conjugation can also occur in CNT–TMO hybrid materials, and similar capacitance enhancement effects are expected, which agrees well with the respective literatures [14,15,22–26]. It is worth pointing out that interfacial conjugation can only be effective if the material structure can facilitate electron and ion conduction, which can result ideally from the functions of CNTs in the composite.

Apparently, to achieve successful interfacial conjugation and maximise its contribution to capacitance enhancement, it is

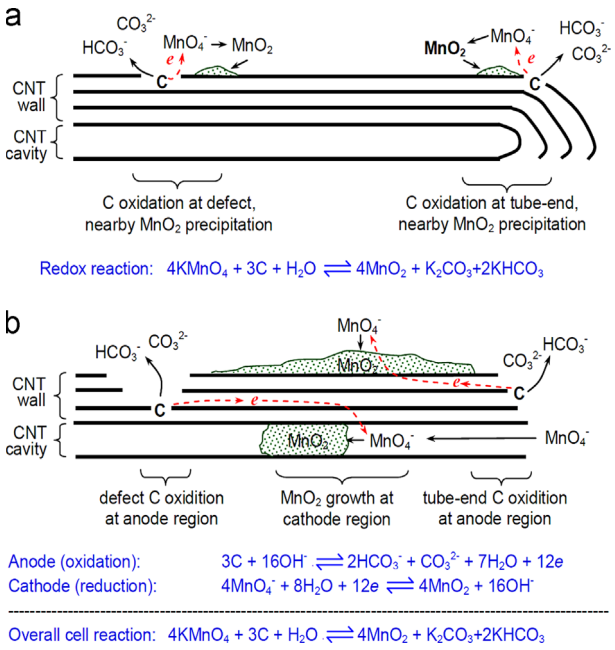

Fig. 9 Mechanism of redox deposition of MnO_2 on CNTs in a neutral aqueous solution, including (a) firstly direct electron transfer from CNT defect and/or tube end to MnO_4^-, leading to MnO_2 precipitation at or near the defect site, and (b) secondly electron transfer from CNT defect and/or tube end through CNT wall and existing MnO_2 coating or filling to MnO_4^- at external or internal surface that is located away from the defect site, leading to growth of nano-crystalline MnO_2 coating and filling [14].

necessary to build an effective interface between CNT and the TMO. An interesting and practically simple approach is through the so called "redox deposition" method [14,27,28]. As a special class of heterogeneous chemical reactions, redox deposition occurs through the oxidation (or reduction) of a solid substrate by an oxidant (or reductant) in a fluid (liquid of gas) to generate a solid product that consequently deposits on the substrate. The following two reactions are typical examples of redox deposition.

Gas/solid (e.g. exposure of titanium to a hot air):

$$\mathrm{Ti(ss)} + \mathrm{O_2(g)} \rightarrow \mathrm{TiO_2(sd/ss)} \tag{10}$$

Liquid/solid (e.g. immersion of graphite in the $KMnO_4$ solution):

$$\mathrm{3C(ss)} + \mathrm{4KMnO_4(l)} + \mathrm{2H_2O(l)} \rightarrow \mathrm{4MnO_2(sd/ss)} + \mathrm{KHCO_3(l)} + \mathrm{K_2CO_3(l)} \tag{11}$$

where ss represents the solid substrate, and sd/ss the solid deposit (sd) on solid substrate.

Redox deposition is highly effective for synthesis of functional hybrid (composite) materials with a particulate or porous substrate precursor. In particular, the reaction and structure formation mechanism of redox deposition was reported for the CNT–MnO_2 hybrids by the author and co-workers as illustrated schematically in Fig. 9.

The CNT/MnO_2 hybrids produced by redox deposition showed typically the core–shell structure as revealed by SEM, TEM and HRTEM in Fig. 10 which also presents the SEM image of CNTs for comparison. It can be seen clearly in Fig. 10 that the MnO_2 coatings are uniform, crystalline, and continuous on the surface of individual CNTs. Such a coherent contact between the shell (MnO_2) and core (CNT) should encourage effective interfacial conjugation, and enhance the capacitance. This prediction is well in line with experimental findings reported in the literature [14,22,29]. Specially, the electrode capacitance of the CNT/MnO_2 composite films was found to increase in proportion to the film thickness, reaching beyond 5 F/cm^2 [14], whilst the charge–discharge performance remained highly stable over 9000 cycles [29].

8. Hybrid nanomaterials with graphenes

In addition to CNTs, graphenes are the focus of many recent research publications on supercapacitors. They are also formed by conjugated bonds, and can therefore contribute to extension of electron delocalisation in ECPs and TMOs. In CNTs, chemical bonds are bent around the axis of the tube, and hence strained to a certain degree against electron delocalisation. Unlike CNTs, graphenes are generally flat with no or little distortion of the conjugated bonds, allowing a greater freedom of the delocalised electrons. Thus, graphenes should be more effective than CNTs for interfacial conjugation when forming hybrids with ECPs or TMOs, and enhance further the pseudo-capacitance. This expectation is in accordance with the reported larger specific capacitance of the graphene–MnO_2 composite (up to 210 F/g) [30] than that of similarly prepared CNT–MnO_2 composite (~140 F/g) [14].

However, this comparison should not lead to the conclusion that graphenes are better than CNTs for supercapacitor applications. This is because the high specific capacitance of a material,

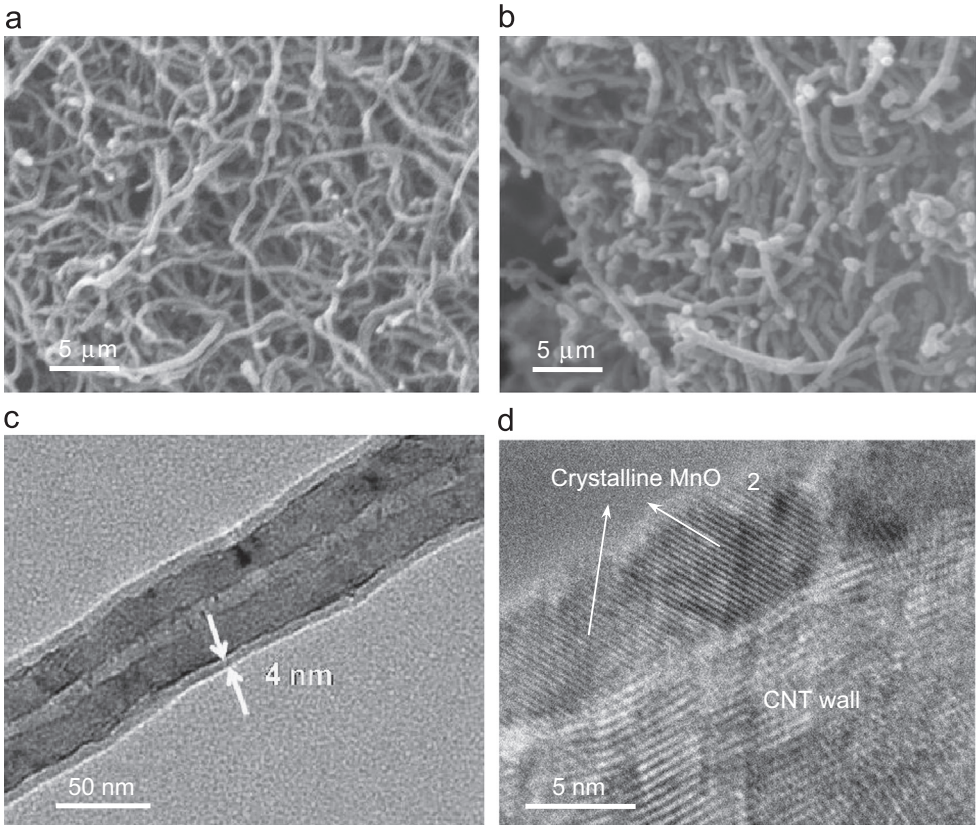

Fig. 10 SEM images of (a) acid treated CNTs and (b) CNT/MnO_2 (30 wt%). (c) TEM image showing a CNT coated with a thin layer (4 nm) of MnO_2. (d) HRTEM image revealing the MnO_2 thin layer to be nano-crystalline on the surface of the CNT. The CNT/MnO_2 samples shown here were prepared by redox deposition as explained in Fig. 9 [14,29].

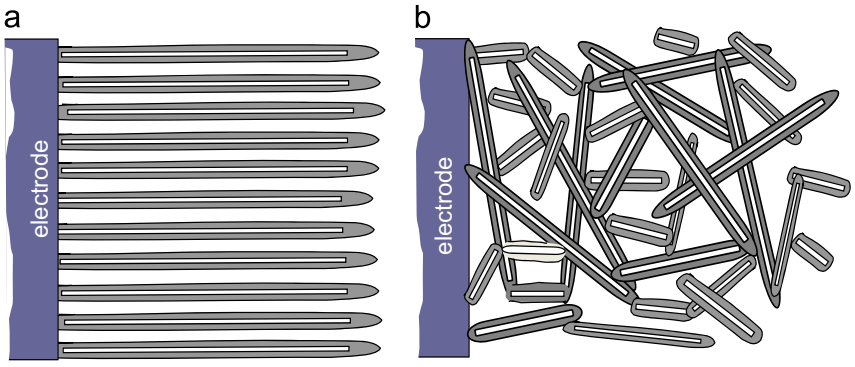

Fig. 11 Arrangement of CNTs on electrode surface via (a) aligned growth and (b) random packing. For making a hybrid material electrode, (a) is usually achieved in two steps: (1) growth of the aligned CNTs, and (2) coating the grown CNTs with a thin layer of TMO or ECP. However, (b) can be achieved in one step, for example, via electro-co-deposition [12,17].

particularly when this property is determined from experiments on small amounts of materials, cannot always be translated into high energy capacity in devices [31].

Instead of being used individually, for supercapacitor and other large-scale device applications, particulates of CNTs and graphenes have to be packed or built into an electrode, or a part of it (e.g. as a coating). As already discussed above, the electrode must have high conductivity for both electrons and ions. For electron conduction, due to the distortion of the chemical bonds in CNTs, it may be predicted that a single-walled CNT may be less conducting than the graphene sheet that has the same dimensions as that resulting from opening (or unzipping) the CNT. However, when present in the electrode, the overall electronic conductivity is more dependent on how percolation is achieved and at what concentration. According to the literature, the lengths of CNTs range typically from several to several tens of micrometres, whilst graphenes are commonly smaller than a micron in either of the two in-plan dimensions. Thus, CNTs should be able to percolate at a lower loading.

Considering ion conduction, both CNTs and graphenes are themselves non-conducting to ions. Therefore, ion conduction in the electrode relies on the number and ionic conductivity of liquid channels that can be introduced into the electrode structure. CNTs can be built into an electrode in two ways to provide effective ion conducting liquid channels as proven experimentally: growing aligned CNTs directly, or packing randomly the CNTs on the electrode surface. These are schematically explained in Fig. 11. Particularly, for curved CNTs, random packing ensures empty spaces between the CNTs. It is also possible to make CNTs into a sufficiently conducting and free-standing film for direct use as the electrode.

While direct growth of aligned graphenes is still a challenge experimentally, random packing of graphenes is the only way reported for making a graphene electrode. Because graphene particulates are thin sheets or plate-like, they can in theory pack into fairly dense structures via face-to-face stacking, at least in a localised manner at microscopic scale. Therefore, random packing of graphenes may not always provide sufficient channels for liquid access and ion conduction.

Based on the analysis above, although qualitative, it can be predicted that ion conduction may be better facilitated in CNTs based electrodes than in graphenes based ones. Such a difference may not affect performance significantly in thin layer electrodes, but is not in favour of ion conduction through, and hence material utilisation in thick films. Although the research on graphenes is still ongoing, up till now, the electrode capacitance of graphene based hybrid materials is typically smaller than 1 F/cm^2, whilst CNT hybrid materials were shown to reach beyond 5 F/cm^2.

9. End remark

The principle and performance governing equations of conventional capacitors have been presented and applied to differentiate between batteries and supercapacitors according the shapes of CVs and GCDs. Particularly, the origin of pseudo-capacitance has been correlated with electron transfer to or from the conduction band of semiconductor type materials, such as ECPs and TMOs, according to the band theory. This understanding confirms that pseudo-capacitance is also featured by rectangular CVs and triangular GCDs. Peak-shaped CVs and non-linear CDs are features of battery behaviour, and should not be used for measurement of capacitance values. Capacitance enhancement is generally expected and observed experimentally in nanostructured materials which however suffer from low conductivity to both electrons and ions. It is shown that the use of CNTs to hybridise with pseudo-capacitance materials is an effective approach to improving electron and ion conduction. A new concept of interfacial conjugation is proposed to reflect the π–π stacking interactions at the interface between CNTs and ECPs or TMOs. It is also shown that although graphenes may be more effective for interfacial conjugation, CNTs are likely more advantageous in networking for electron conduction and forming porous structures for ion conduction. In other words, CNT hybrid materials are practically more attractive for development of thick electrode films, and hence high energy capacity devices.

Acknowledgement

Since 2000, the author and more than 20 co-workers whose names appear in the list of references have researched on various aspects of supercapacitors, and received financial support from the EPSRC, Royal Society, MOSTI, E.ON AG (International Research Initiative—Energy Storage 2007), and Season Long Cleantech Ltd (Beijing). Responsibility for the content of this publication lies with the author.

References

[1] A. Rufer, P. Barrade, IEEE Transactions on Industry Applications 38 (2002) 1151–1159.

[2] H.L. Wang, H.S. Casalongue, Y.Y. Liang, H.J. Dai, Journal of the American Chemical Society 132 (2010) 7472–7477.
[3] P.A. Mini, A. Balakrishnan, S.V. Nair, K.R.V. Subramanian, Chemical Communications 47 (2011) 5753–5755.
[4] D.-D. Zhao, M.W. Xu, W.-J. Zhou, J. Zhang, H.L. Li, Electrochimica Acta 53 (2008) 2699–2705.
[5] H. Zhang, G. Cao, Y. Yang, Energy and Environmental Science 2 (2009) 932–943.
[6] B. Howard, Patent no. US2800616, 1957.
[7] J. Miller, Batteries and energy storage technology, Autumn (2007) 61–78 ⟨http://bestmag.co.uk/⟩.
[8] S. Trasatti, G. Buzzanca, Journal of Electroanalytical Chemistry 29 (1971) A1–A5.
[9] J.H. Chae, K.C. Ng, G.Z. Chen, Proceedings of the Institution of Mechanical Engineers—Part A: Journal of Power Engineering 224 (2010) 479–503.
[10] S.W. Zhang, G.Z. Chen, Energy Materials 3 (2008) 186–200.
[11] A.J. Bard, L.R. Faulkner, Electrochemical Methods: Fundamentals and Applications, John Wiley & Sons, New York, 2001.
[12] G.Z. Chen, M.S.P. Shaffer, D. Coleby, G. Dixon, W.Z. Zhou, A.H. Windle, D.J. Fray, Advanced Materials 12 (2000) 522–526.
[13] C. Peng, G.A. Snook, D.J. Fray, M.S.P. Shaffer, G.Z. Chen, Chemical Communications (2006) 4629–4631.
[14] X.B. Jin, W.Z. Zhou, S.W. Zhang, G.Z. Chen, Small 3 (2007) 1513–1517.
[15] K.C. Ng, S.W. Zhang, C. Peng, G.Z. Chen, Journal of the Electrochemical Society 156 (2009) A846–A853.
[16] X.H. Zhou, G.Z. Chen, Journal of the Electrochemical 18 (2012) 548–564, 〈http://electrochem.xmu.edu.cn/EN/volumn/home.shtml〉.
[17] C. Peng, J. Jin, G.Z. Chen, Electrochimica Acta 53 (2007) 525–537.
[18] M.Q. Wu, G.A. Snook, V. Gupta, M. Shaffer, D.J. Fray, G.Z. Chen, Journal of Materials Chemistry 15 (2005) 2297–2303.
[19] M. Hughes, G.Z. Chen, M.S.P. Shaffer, D.J. Fray, A.H Windle, Chemistry of Materials 14 (2002) 1610–1613.
[20] G.A. Snook, G.Z. Chen, D.J. Fray, M. Hughes, M. Shaffer, Journal of Electroanalytical Chemistry 568 (2004) 135–142.
[21] J. Huang, X. Li, J. Xu, H. Li, Carbon 41 (2003) 2731–2736.
[22] S.-B. Ma, K.-W. Nam, W.-S. Yoon, X.-Q. Yang, K.-Y. Ahn, K.-W. Oh, K.-B. Kim, Journal of Power Sources 178 (2008) 483–489.
[23] W.-D. Zhang, B. Xu, L.-C. Jiang, Journal of Materials Chemistry 20 (2010) 6383–6391.
[24] W.-C. Fang, Journal of Physical Chemistry C 112 (2008) 11552–11555.
[25] Y. Shan, L. Gao, Materials Chemistry and Physics 103 (2007) 206–210.
[26] J.-S. Ye, H.F. Cui, X. Liu, T.M. Lim, W.-D. Zhang, F.-S. Sheu, Small 1 (2005) 560–565.
[27] M.Q. Wu, G.A. Snook, G.Z. Chen, D.J. Fray, Electrochemistry Communications 6 (2004) 499–504.
[28] M.B. Sassin, C.N. Chervin, D.R. Rolison, J.W. Wang, Accounts of Chemical Research (2012), http://dx.doi.org/10.1021/ar2002717.
[29] S.W. Zhang, C. Peng, K.C. Ng, G.Z. Chen, Electrochimica Acta 55 (2010) 7447–7453.
[30] S. Chen, J.W. Zhu, X.D. Wu, Q.F. Han, X. Wang, ACS Nano 4 (2010) 2822–2830.
[31] G.A. Snook, C. Peng, D.J. Fray, G.Z. Chen, Electrochemistry Communications 9 (2007) 83–88.

George Zheng Chen (http://www.nottingham.ac.uk/~enzgzc), FRSC, FRSA, FIMMM, is professor of University of Nottingham. He obtained his Ph.D. degree from University of London (supervised by Prof. W. John Albery in Imperial College) in Physical Chemistry in 1992, and worked previously in Universities of Cambridge, Leeds and Oxford, and Wuhan and Jiangxi (now Nanchang) Universities. His research aims at electrochemical and liquid salts innovations for materials, energy and environment, producing 18 patents (including the Fray-Farthing-Chen Cambridge Process), 60 Ph.D. and M.Sc. theses, 154 articles in peer reviewed journals and books, and over 270 invited and contributed presentations at conferences and seminars.